Frequency selectivity in Old-World monkeys corroborates sharp cochlear tuning in humans

Philip X. Joris[a,1], Christopher Bergevin[b,1], Radha Kalluri[c], Myles Mc Laughlin[a], Pascal Michelet[a], Marcel van der Heijden[a], and Christopher A. Shera[c,2]

[a]Laboratory of Auditory Neurophysiology, University of Leuven, BE-3000 Leuven, Belgium; [b]Department of Mathematics, University of Arizona, Tucson, AZ 85721; and [c]Eaton–Peabody Laboratories, Harvard Medical School, Boston, MA 02114

Edited by Michael Merzenich, W. M. Keck Center for Integrative Neuroscience, University of California, San Francisco, CA, and approved September 7, 2011 (received for review April 12, 2011)

Frequency selectivity in the inner ear is fundamental to hearing and is traditionally thought to be similar across mammals. Although direct measurements are not possible in humans, estimates of frequency tuning based on noninvasive recordings of sound evoked from the cochlea (otoacoustic emissions) have suggested substantially sharper tuning in humans but remain controversial. We report measurements of frequency tuning in macaque monkeys, Old-World primates phylogenetically closer to humans than the laboratory animals often taken as models of human hearing (e.g., cats, guinea pigs, chinchillas). We find that measurements of tuning obtained directly from individual auditory-nerve fibers and indirectly using otoacoustic emissions both indicate that at characteristic frequencies above about 500 Hz, peripheral frequency selectivity in macaques is significantly sharper than in these common laboratory animals, matching that inferred for humans above 4–5 kHz. Compared with the macaque, the human otoacoustic estimates thus appear neither prohibitively sharp nor exceptional. Our results validate the use of otoacoustic emissions for noninvasive measurement of cochlear tuning and corroborate the finding of sharp tuning in humans. The results have important implications for understanding the mechanical and neural coding of sound in the human cochlea, and thus for developing strategies to compensate for the degradation of tuning in the hearing-impaired.

auditory filters | comparative hearing

Sound waveforms consist of pressure fluctuations in time and space. In the process of transducing mechanical vibrations into neural signals, the cochlea performs a mechanical frequency analysis that decomposes sounds into constituent frequencies (1, 2). The frequency tuning of the cochlear filters plays a critical role in the ability to distinguish and segregate different sounds perceptually. For example, sounds that radiate from different sources superpose in the air, and are thus "mixed up" before striking the eardrums. Based on the output of the cochlear filters, and by comparing responses from the two ears, the nervous system is capable of disentangling the various sounds, grouping related frequency components to identify auditory objects and localize their sources in space (3). The critical role of peripheral frequency selectivity is perhaps best illustrated by the consequences of damage to the inner ear, which typically leads to a degradation of the cochlear filters. The loss of sharp filtering results in an impaired ability to detect signals in noise and to separate different sounds (4). Frequency selectivity is therefore crucial to everyday human communication.

The study of the cochlea is hampered by its fragility and inaccessibility. Direct measurements of mechanical or neural frequency tuning in healthy cochleae are only possible in laboratory animals. To date, measurements of the mechanical vibration of the cochlea's basilar membrane have been largely restricted to the basal high-frequency end of the cochlea, where surgical access is convenient (2). Recordings from individual auditory-nerve fibers (5–7) enable a detailed characterization of the frequency channels set up along the entire length of the cochlea (8–14), but they too are surgically invasive. Although direct measurements are not possible in humans, neural recordings indicate that cochlear tuning is generally similar across common laboratory animals (15); tuning in humans has therefore long been regarded as comparable.

A promising alternative procedure allows the objective noninvasive estimation of cochlear tuning, and can therefore be applied to humans (16, 17). As a byproduct of the tuned mechanical amplification responsible for the ear's impressive sensitivity and dynamic range, the cochlea emits sound in response to sound (18). The delays (latencies) of the sounds evoked from the ear by pure tones, sounds known as stimulus-frequency otoacoustic emissions (SFOAEs), provide a measure of the mechanical delay within the cochlea (19, 20). Across a wide variety of animals ranging from mammals to lizards, SFOAE delays appear well correlated with the sharpness of neural tuning (16, 17, 21), a correlation consistent both with models of emission generation (21–23) and with relationships between tuning and delay expected from filter theory (24). Consistent with the time-frequency uncertainty principle, filters with narrower bandwidths (i.e., more well-defined center frequencies) generally have longer group delays (i.e., impulse responses that are more spread out in time).

Interestingly, humans have the longest SFOAE delays of any species so far examined. Because filter theory associates longer delay with sharper tuning, human emission latencies have been interpreted as indicative of sharper tuning. An extension of this reasoning, based on the assumption that the relationship between SFOAE delay and neural tuning manifest in laboratory animals extends to other mammals, allows one to obtain quantitative estimates of neural tuning from otoacoustic measurements (16, 17). When applied to humans, the method yields tuning estimates that coincide with behavioral values obtained using revised psychophysical paradigms designed to mimic the measurement of neural tuning curves (25). Nevertheless, because they suggest that human cochlear tuning is substantially sharper than that of common laboratory animals, the reliability of the otoacoustic and behavioral estimates, as well as their apparent consequences for the exceptionality of the human cochlea, have been questioned and remain controversial (15,26–28).

Results

We measured both otoacoustic emissions and auditory-nerve responses in two species of macaque monkeys. As Old-World primates, macaques are more closely related to humans than are the common laboratory animals generally used in studies of frequency selectivity. Our goal was thus to explore the apparent

Author contributions: P.X.J., C.B., R.K., M.v.d.H., and C.A.S. designed research; P.X.J., C.B., R.K., M.M.L., P.M., M.v.d.H., and C.A.S. performed research; P.X.J., C.B., R.K., M.M.L., P.M., M.v.d.H., and C.A.S. analyzed data; and P.X.J. and C.A.S. wrote the paper.

The authors declare no conflict of interest.

This article is a PNAS Direct Submission.

[1]P.X.J. and C.B. contributed equally to this work.

[2]To whom correspondence should be addressed. E-mail: shera@epl.meei.harvard.edu.

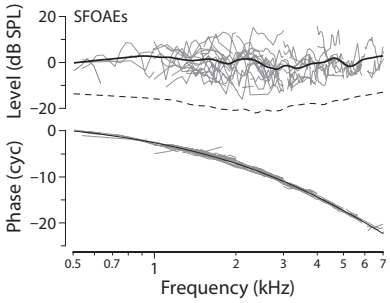

Fig. 1. SFOAEs in macaques. (*Upper*) SFOAE level (gray lines) and their loess trend (black line) vs. frequency measured at a sound-pressure level (SPL) of 40 dB in 24 ears (21 rhesus macaques, *M. mulatta*). Only data points at least 10 dB above the noise are shown (dashed line is the average noise floor). (*Lower*) Corresponding unwrapped phases (gray lines) and their trend (black line), constructed by integrating the trend line for the delay (Fig. 2). As explained in *Materials and Methods*, SFOAEs were measured in discrete segments spanning 0.5–1 kHz. To emphasize the robustness of the trend in the phase slope, individual phase segments were shifted vertically by an integral number of cycles (cyc) to lie closer to the trend.

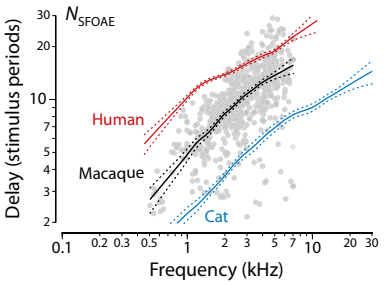

Fig. 2. SFOAE delays in macaques compared with other species. Gray dots and trend (black line with flanking dots delimiting 95% confidence intervals in the central tendency) show macaque phase-gradient (group) delays, N_{SFOAE}, in periods of the stimulus frequency computed from the data in Fig. 1. Blue and red lines show published species trends in cats and humans (20).

exceptionality of the human cochlea while providing a direct test of the noninvasive method for estimating cochlear tuning.

Otoacoustic Delays in Macaques Are Intermediate Between Those in Cats and Humans. SFOAEs are sinusoids at the stimulus frequency. Fig. 1 shows measurements of SFOAE magnitude and phase vs. frequency in 21 rhesus macaques. Evidently, macaques produce SFOAEs with levels comparable to those reported in normal-hearing humans and other mammals. SFOAE phase in macaques falls through many cycles, resembling that measured in other mammals and indicating a substantial delay arising within the cochlea.* As computed from the gradient of the phase, macaque SFOAE delays decrease from about 4 ms at 0.5 kHz to about 2 ms at 7 kHz. Fig. 2 shows SFOAE delays in the dimensionless form, N_{SFOAE}, representing the delay in periods of the stimulus frequency. The trend across frequency is quite robust; the scatter apparent in the data is typical of SFOAEs and does not arise from pathology or measurement noise (the measurements are quite reproducible) but reflects the role of mechanical irregularity inherent in the process of emission generation (22).

As shown in Fig. 2, SFOAE delays in macaques appear intermediate between those in humans and cats or other common laboratory animals.† Although closer to delays measured in cats at frequencies below 1 kHz, N_{SFOAE} values in the macaque approach the longer human values at higher frequencies (note the logarithmic ordinate). If SFOAE delays reflect the bandwidths of frequency filtering within the cochlea, as previously suggested (16, 17), the otoacoustic measurements indicate that the sharpness of tuning in macaques is broader than in humans at low frequencies but more similar at high frequencies.

Auditory-Nerve Tuning in Macaques Is Sharper than in Common Laboratory Animals. The only published data from single auditory-nerve fibers in Old-World monkeys (various macaque species) date from almost half a century ago (6, 7). Unfortunately, these pioneering studies, which are among the first single-fiber recordings in the auditory nerve of any mammal, do not report measures on sharpness of tuning as such, and the tuning curves shown are too limited in number, characteristic frequency (CF) range, and resolution to assess frequency tuning relative to common laboratory animals. We recorded from single auditory-nerve fibers in 16 macaque monkeys (10 *Macaca fascicularis* and 6 *Macaca mulatta*). For each recorded axon, we determined the spontaneous rate, tracked the threshold sound intensity over a range of frequencies, and determined the frequency of lowest threshold (CF) (8). No systematic differences between the two species were found, and the data were therefore pooled. Fig. 3 shows a representative selection of macaque tuning curves. As in other mammals, tuning curves are generally V-shaped and become narrower with increasing CF when plotted on a logarithmic frequency axis. Also shown are the thresholds at CF for all fibers (symbols). The lower envelope of these data (dashed curve) is reasonably consistent with behavioral threshold measurements for pure tones (32). No systematic differences were found in thresholds or tuning bandwidths for fibers differing in spontaneous rate. Only the most sensitive fibers, those with CF thresholds within 30 dB of the dashed curve, were used in the subsequent analysis.

To quantify the sharpness of tuning, we derived the equivalent rectangular bandwidth (ERB) and the corresponding dimensionless quality factor (Q_{ERB} = CF/ERB) from each neural tuning curve. The ERB is a parameter-free measure of tuning equal to the bandwidth of the rectangular filter with the same peak amplitude that passes the same total power in response to white noise. Larger Q_{ERB} values indicate sharper frequency selectivity. Fig. 4 shows macaque Q_{ERB} values (gray dots) and their trend with CF (black line) compared both with species trends from neural measurements in cats (blue) and with the human otoacoustic and behavioral values (red) from the studies discussed above (16, 17, 25). The species trends appear consistent with expectations based on the values of N_{SFOAE} (Fig. 2). In particular, Q_{ERB} values in cats and monkeys overlap at the lowest CFs but separate above 500–1000 Hz, where tuning in macaques becomes twice as sharp as in cats. At the highest frequencies (CF > 4–5 kHz), auditory-nerve tuning in macaque monkeys matches the values previously estimated for humans on the basis of otoacoustic measurements.

Otoacoustic Estimates of Tuning Match the Neural Values. The otoacoustic and neural data in macaques can be combined to provide a quantitative test of the otoacoustic method for estimating cochlear tuning. The otoacoustic method (17) indicates that approximate trend values of Q_{ERB} in macaques can be obtained from measurements of SFOAE delay using the formula:

$$Q_{ERB}(CF) \cong r\,(CF/CF_{a|b})N_{SFOAE}(f)|_{f=CF} \quad [1]$$

In this equation, r is an empirically determined proportionality function known as the tuning ratio (17). $CF_{a|b}$ is the apical-basal transition CF, a species-dependent parameter defined by the ob-

*Although middle-ear transmission has not been measured in macaques, studies in other mammals suggest that delays attributable to round-trip middle-ear transmission appear negligible compared with traveling-wave delay (29–31).

†Otoacoustic delays and neural tuning in guinea pigs and chinchillas are generally similar to those in cats (17, 20).

NEUROSCIENCE

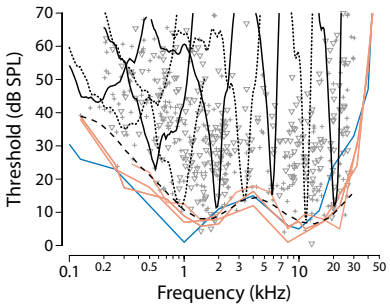

Fig. 3. Example auditory-nerve tuning curves in macaques. The nine tuning curves shown were selected for completeness over a wide range of sound-pressure levels, for sensitivity near the lower limit of the population, and for approximately geometric CF spacing. For clarity, tuning curves are shown by alternating solid and dashed lines. Gray symbols indicate thresholds at CF for fibers with high (+) or low (▿) spontaneous rates (above or below 18 spikes per second, respectively) for all 496 recorded fibers. The dashed line shows the smoothed lower envelope of the neural threshold data. Behavioral thresholds from four studies (32) are shown in orange (*M. mulatta*) and blue (*M. fascicularis*).

servation that the cochleae of many mammalian species appear to divide naturally into two parts: a high-frequency region of apparently basal-like behavior ($CF > CF_{a|b}$) and a low-frequency region of more apical-like behavior ($CF < CF_{a|b}$). The approximate value of $CF_{a|b}$ can be estimated from the location of the bend in the N_{SFOAE} curve (Fig. 2). Previous work has shown that tuning ratios r ($CF/CF_{a|b}$) in cats, guinea pigs, and chinchillas can be well approximated by a single common curve (17). The procedure applied here assumes that this approximate species-invariance of r extends to macaques, and we therefore use the average of the tuning ratios reported for cats, guinea pigs, and chinchillas (17). The parameter $CF_{a|b}$ for macaques was taken as 1.7 kHz, intermediate between the transition CFs previously estimated for cats (in the range of 3–4 kHz) and humans (in the range of 1–1.5 kHz). Our estimate of $CF_{a|b}$ is not critical; varying its value by half an octave in either direction has relatively minor effects on the results.

Fig. 4 shows the estimated values of Q_{ERB} (dashed black line) computed from Eq. **1** using the N_{SFOAE} measurements from Fig. 2. The agreement with the direct neural measurements of Q_{ERB} is excellent. The otoacoustic method reproduces both the overall sharpness and frequency dependence of cochlear tuning, providing reliable values of the Q_{ERB} trend over the full range for which predicted values can be compared with the neural recordings.

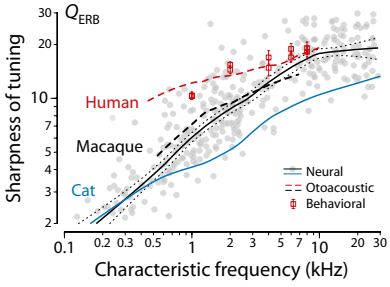

Fig. 4. Sharpness of tuning in macaques and other species. Gray dots and trend (black line with flanking dots delimiting 95% confidence intervals for the trend) show macaque Q_{ERB} values derived from auditory-nerve tuning curves with qualifying thresholds (n = 385). The blue line shows the neural trend in cats (ensemble data from the University of Leuven laboratory and those of M. C. Liberman and B. Delgutte); confidence intervals for the cat trend (not shown for clarity) are smaller than those for the monkey. The red dashed line gives the human trend previously derived from SFOAE delay (16, 17); the red squares and SEs show revised behavioral values (25). The black dashed line gives the macaque Q_{ERB} trend obtained from Eq. **1** using the values of N_{SFOAE} in Fig. 2.

Discussion

By themselves, the neural data demonstrate that at CFs greater than about 500 Hz, the two species of macaques examined here have significantly sharper cochlear tuning than the laboratory animals for which frequency tuning has been most extensively studied (cats, guinea pigs, and chinchillas). The data provide an important counterexample to the common notion that the sharpness of cochlear tuning is essentially the same in all mammalian species, including humans (15). In particular, the neural data indicate that at CFs above 4–5 kHz, cochlear tuning in Old-World monkeys can be just as sharp as previously derived for humans (16, 25). With the proper comparison, the human otoacoustic estimates are neither prohibitively sharp nor exceptional. Evidently, the inner ears of macaques and humans differ from those of common laboratory animals in their most fundamental capacity as a frequency analyzer.

When combined with recent reports of sharp frequency tuning in the auditory cortex of marmosets, macaques, and humans (33–35), our results support the conjecture that fine auditory frequency resolution, like high visual acuity (36, 37), may be characteristic of primates more generally. However, far too few mammalian species have been studied by either behavioral, otoacoustic, or physiological methods to allow broad conclusions regarding relative tuning bandwidths in primates. Even restricting the discussion to our closest primate relatives, there remain several hundred extant simian species. These species range over three orders of magnitude in body mass and live out their lives in a vast array of habitats. Although phylogenetic constraints must play a role in determining the sharpness of cochlear tuning, so must the acoustical environments and vocal behaviors of individual species in the lineage. Both species-specific adaptations to a diversity of signal-processing requirements and cochlear structural parameters that presumably vary among primates can have significant effects on peripheral frequency tuning. A simple example of such a parameter is the space constant of the cochlear tonotopic map and its correlation with the length of the basilar membrane (17).

Although the narrow tuning bandwidths recently reported in single neurons of the human auditory cortex (33) are, in fact, similar to the otoacoustic and behavioral values previously derived (16, 25) for the human auditory nerve (Fig. 4), it remains unclear to what extent sharp frequency tuning at higher anatomical levels reflects cochlear mechanisms, even for the few mammalian species for which data are available. In New-World monkeys, sharp tuning (relative to cats) is present at cortical and thalamic levels (34) but not at the periphery (15, 38, 39). In macaques and humans, there is now evidence for sharp frequency tuning at both cortical (33, 35) and cochlear levels (this report and ref. 16). Quite independent of the phylogenetic issue, our studies allow the parsimonious statement that human auditory behavior should be modeled with sharper cochlear filters than suggested by work on the cat, guinea pig, and chinchilla.

Our study was motivated, in part, by the earlier suggestion that cochlear tuning in macaques might be substantially sharper than in cats and guinea pigs (16), a suggestion based on SFOAE measurements in rhesus macaques near 2 kHz (40). At CFs above about 500 Hz, the neural data verify that macaques do indeed have sharper cochlear tuning, as suggested; at lower frequencies, however, their tuning appears comparable to that of other laboratory animals. This combination of results was unexpected because it implies that the variation of the sharpness of tuning across CFs is greater in macaques than that so far encountered in other mammals. Put another way, the mean slope on log-log axes of the function Q_{ERB} vs. CF is larger in macaques than in cats, guinea pigs, chinchillas, and humans (Fig. 4), species in which the slopes are all similar (20). As shown in Fig. 2, steeper slopes in macaques are characteristic not only of the neural measurements of Q_{ERB} but of the otoacoustic measurements of N_{SFOAE}. Although their un-

usual frequency dependence makes Q_{ERB} and N_{SFOAE} appear exceptional in macaques, together, they prove the rule that the ratio of the two variables (i.e., tuning ratio $r = Q_{ERB}/N_{SFOAE}$) varies much less than either quantity individually while remaining relatively invariant across species. Covariation of Q_{ERB} and N_{SFOAE} across frequency is consistent with relationships between tuning and delay expected from filter theory (16, 17).

We emphasize that the direct measures of neural tuning reported here are quantitatively consistent with the indirect estimates obtained using measurements of SFOAE delay (Fig. 4). Together, our two datasets validate the otoacoustic method and corroborate revised psychophysical procedures (25) as reliable means to assess the sharpness of cochlear tuning noninvasively. This finding, even more than the argument based on phylogenetic proximity of macaques and humans, reinforces the case for sharp cochlear tuning in humans. In addition to its application in humans, the otoacoustic method enables the objective assessment of cochlear tuning in other animals for which invasive recordings are undesirable, impractical, or prohibited. One obvious application would be the noninvasive exploration of cochlear tuning in other primate species (41).

Another line of experimentation possible in humans combines masking paradigms with measurement of gross neural potentials (i.e., the compound action potential) recorded in the middle ear. To date, studies have yielded mixed results, with some finding that human tuning appears similar to that of cats and guinea pigs (42) and others finding that human tuning is significantly sharper (43, 44). Technical issues regarding masking paradigms aside (15, 17, 25), a general concern with these studies is that they were conducted in human subjects with impaired hearing. Compound action potential recordings using identical masking paradigms in both experimental animals and humans with normal hearing offer a promising tool for bridging our understanding of cochlear tuning across species.

The implications of differences in peripheral frequency selectivity in humans compared with common laboratory animals are pervasive. For example, the neural bases for human perceptual abilities, such as frequency or vowel discrimination, over a large range of intensities are poorly understood and much debated (45, 46), but quantitative models are invariably based on the frequency selectivity measured in other animals. The debate as to whether cochlear frequency selectivity is insufficiently sharp and needs to be complemented with a temporal code to operate over the greater than 100-dB range of intensities over which humans hear is fundamental to the understanding of the effects of cochlear pathology, and thus for developing algorithms for auditory prostheses to relieve hearing loss and deafness.

Finally, although our discussion has emphasized differences in tuning and delay among species, the success of the otoacoustic method in cats, guinea pigs, chinchillas, macaques, and humans indicates that many mammalian cochleae appear almost identical in one fundamental respect: After compensating for differences between apical and basal regions of the cochlea (through the value of $CF_{a|b}$), all five species examined to date have nearly the same tuning ratio, r. (If tuning ratios in macaques differed significantly from those in cats, guinea pigs, and chinchillas, the otoacoustic estimates of Q_{ERB} would not match the neural measurements.) Thus, although the sharpness of tuning and otoacoustic delay may vary widely across species, the curve representing their ratio ($r = Q_{ERB}/N_{SFOAE}$) remains almost invariant (17). The near species-invariance of the tuning ratio suggests that despite their many differences, these and perhaps all mammals implement similar types of filters at corresponding locations in their cochleae (17).

Materials and Methods

All procedures performed at the Massachusetts Institute of Technology (MIT) were approved by the MIT Institutional Animal Care and Use Committee; those performed at the University of Leuven were approved by the Ethics Committee for Animal Experiments.

Otoacoustic Measurements. We measured otoacoustic emissions in 21 healthy adult rhesus macaques (*M. mulatta*) while they were anesthetized for routine veterinary care at MIT. The monkeys were members of a colony used for nonauditory neurophysiological studies; their ages ranged from 4 to 22 y, and their weights ranged from 4 to 15 kg. Although behavioral audiograms are not available for the monkeys, their emission levels were comparable to those measured in other mammals with normal hearing, including humans. The monkeys were anesthetized with Telazol (5 mg/kg) and received maintenance doses of Telazol (2.5 mg/kg) or ketamine (5 mg/kg) as needed. We measured SFOAEs using the suppression method (47–49) implemented on the Mimosa Acoustics measurement system, which employs the Etymōtic Research ER10c probe. Probe and suppressor sound-pressure levels (SPLs) were 40 and 55 dB, respectively. System distortion limited the measurements to probe frequencies less than about 7 kHz. Because the monkeys were only lightly anesthetized and could awaken with little warning and much commotion, we organized the measurements into short-frequency segments spanning intervals of 0.5–1 kHz. The light anesthesia also elevated the noise floor, which varied across animals. Only data at least 10 dB above the noise floor were included in subsequent analysis.

Auditory-Nerve Recording. We obtained auditory-nerve recordings from 753 single fibers in 16 macaque monkeys (10 *M. fascicularis* and 6 *M. mulatta*) using methods routinely applied for similar recordings in cats at our laboratory at the University of Leuven (10, 50). The animals were juveniles and adults of both sexes; their weights averaged 5.5 kg (range: 1.6–10.5 kg). Some animals had been used in nonauditory neurophysiological studies. Animals were placed in a double-walled sound-attenuating booth and given an infusion of 5% (wt/vol) dextrose (i.v.); vital signs were continuously monitored throughout the recording session. Using a posterior fossa approach under deep barbiturate anesthesia (pentobarbital, 25 mg/kg), the lateral cerebellum was retracted and partially removed to expose the auditory and vestibular nerves. A recording chamber supporting a hydraulic microdrive was glued to the skull. Recording electrodes (3-M KCl or NaCl pipettes, impedance ~40 MΩ) were visually positioned peripheral to the Schwann-glia border. Sounds were delivered with a dynamic speaker and compensated digitally for the acoustic transfer function measured in the ear canal with a probe microphone. After isolating a single fiber, we measured spontaneous rate over a 15-s silent period and obtained threshold tuning curves using a two-down one-up tracking paradigm with the frequency step size adjusted for CF (in octaves, from 0.15 at the lowest CFs to 0.01 at the highest). To remove noise attributable to the tracking algorithm, we applied Savitzky–Golay smoothing filters to the sample tuning curves shown in Fig. 3. We obtained complete datasets from 496 different fibers.

Our sample of tuning curves in cats derives from all animals studied during the same time period as the monkeys. The distribution of tuning sharpness we obtained in cats is nearly coincident with a large independent sample obtained in the laboratories of other investigators (courtesy of M. C. Liberman and B. Delgutte, Harvard Medical School, Boston MA). The total sample consists of more than 2,500 fibers. We took care to apply the same experimental and analysis protocol to the neural recordings in monkeys that we do in cats. One procedural difference, however, was that recordings from the monkey auditory nerve were discontinued only when thresholds in both ears were clearly pathological or when mechanical instability prevented single-unit recording. Although the lowest neural thresholds were close to behavioral thresholds reported for the two macaque species studied (32) (Fig. 3), thresholds were often higher than expected, with large interanimal variation. This may be related to the difficulty of obtaining reliable acoustic calibration at high frequencies because of the long and narrow bony ear canal (39) and perhaps to vasospasm or other trauma induced by surgical exposure of the VIIIth nerve (51). Variability in neural thresholds is also observed in cats (8) but only rarely to the extent encountered in the monkeys. Because increases in threshold are typically accompanied by decreases in frequency selectivity (1, 2), only tuning curves with CF thresholds within 30 dB of the best threshold curve computed from the population were used in the Q_{ERB} analysis for both monkeys and cats. Varying the selection criteria had essentially no effect on the trend or conclusions. Nevertheless, because our sampling from monkeys includes elevated thresholds, whereas the sampling from cats does not, our estimates of the relative sharpness of tuning in the macaques are probably conservative.

Analysis. SFOAE phases were corrected for the approximate acoustic delay attributable to the distance between the microphone and tympanic membrane (estimated at about 1.2 cm), and acoustic calibrations removed delays introduced by the measurement system. Measurement frequency resolution was sufficient to resolve ambiguities attributable to phase unwrapping. Phase-gradient delays were computed from the slope of the unwrapped

phase (Fig. 1) using centered differences (20). ERBs were computed from the neural tuning curves using standard algorithms. Otoacoustic and neural trend lines were computed using locally linear regression (robust loess), with confidence intervals determined using bootstrap resampling.

ACKNOWLEDGMENTS. We thank Robert Marini, the MIT veterinary staff, and the MIT and Leuven investigators who graciously allowed us access to their monkeys for the measurements. B. Delgutte, J. J. Guinan, M. C. Liberman, G. Zweig, and the anonymous reviewers provided helpful comments on the manuscript. Work in Belgium was supported by the Fund for Scientific Research–Flanders (Grants G.0392.05 and G.0633.07) and Research Fund of the University of Leuven (Grants OT/01/42 and OT/05/57). Work in the United States was supported by the Howard Hughes Medical Institute (Grant 52003749), National Science Foundation Division of Mathematical Sciences (Grant 0602173), and National Institutes of Health (Grant R01 DC003687 to C.A.S.).

1. Dallos P (1996) *The Cochlea*, eds Dallos P, Popper AN, Fay RR (Springer, New York), pp 1–43.
2. Robles L, Ruggero MA (2001) Mechanics of the mammalian cochlea. *Physiol Rev* 81: 1305–1352.
3. Bregman AS (1990) *Auditory Scene Analysis: The Perceptual Organization of Sound* (MIT Press, Cambridge, MA).
4. Peters RW, Moore BCJ, Baer T (1998) Speech reception thresholds in noise with and without spectral and temporal dips for hearing-impaired and normally hearing people. *J Acoust Soc Am* 103:577–587.
5. Kiang NYS, Watanabe T, Thomas EC, Clark LF (1965) *Discharge Patterns of Single Fibers in the Cat's Auditory Nerve* (MIT Press, Cambridge, MA).
6. Katsuki Y, Kanno Y, Suga N, Mannen M (1961) Primary auditory neurons of monkey. *Jpn J Physiol* 11:678–683.
7. Nomoto M, Suga N, Katsuki Y (1964) Discharge patterns and inhibition of primary auditory nerve fibers in the monkey. *J Neurophysiol* 27:768–787.
8. Liberman MC (1978) Auditory-nerve response from cats raised in a low-noise chamber. *J Acoust Soc Am* 63:442–455.
9. Kim DO, Molnar CE, Matthews JW (1980) Cochlear mechanics: Nonlinear behavior in two-tone responses as reflected in cochlear-nerve-fiber responses and in ear-canal sound pressure. *J Acoust Soc Am* 67:1704–1721.
10. van der Heijden M, Joris PX (2003) Cochlear phase and amplitude retrieved from the auditory nerve at arbitrary frequencies. *J Neurosci* 23:9194–9198.
11. van der Heijden M, Joris PX (2006) Panoramic measurements of the apex of the cochlea. *J Neurosci* 26:11462–11473.
12. Recio-Spinoso A, Temchin AN, van Dijk P, Fan YH, Ruggero MA (2005) Wiener-kernel analysis of responses to noise of chinchilla auditory-nerve fibers. *J Neurophysiol* 93: 3615–3634.
13. Shera CA (2007) Laser amplification with a twist: Traveling-wave propagation and gain functions from throughout the cochlea. *J Acoust Soc Am* 122:2738–2758.
14. Temchin AN, Rich NC, Ruggero MA (2008) Threshold tuning curves of chinchilla auditory-nerve fibers. I. Dependence on characteristic frequency and relation to the magnitudes of cochlear vibrations. *J Neurophysiol* 100:2889–2898.
15. Ruggero MA, Temchin AN (2005) Unexceptional sharpness of frequency tuning in the human cochlea. *Proc Natl Acad Sci USA* 102:18614–18619.
16. Shera CA, Guinan JJ, Jr., Oxenham AJ (2002) Revised estimates of human cochlear tuning from otoacoustic and behavioral measurements. *Proc Natl Acad Sci USA* 99: 3318–3323.
17. Shera CA, Guinan JJ, Jr., Oxenham AJ (2010) Otoacoustic estimation of cochlear tuning: Validation in the chinchilla. *J Assoc Res Otolaryngol* 11:343–365.
18. Kemp DT (1978) Stimulated acoustic emissions from within the human auditory system. *J Acoust Soc Am* 64:1386–1391.
19. Kemp DT (1986) Otoacoustic emissions, travelling waves and cochlear mechanisms. *Hear Res* 22:95–104.
20. Shera CA, Guinan JJ, Jr. (2003) Stimulus-frequency-emission group delay: A test of coherent reflection filtering and a window on cochlear tuning. *J Acoust Soc Am* 113: 2762–2772.
21. Bergevin C, Shera CA (2010) Coherent reflection without traveling waves: On the origin of long-latency otoacoustic emissions in lizards. *J Acoust Soc Am* 127: 2398–2409.
22. Shera CA, Tubis A, Talmadge CL (2008) Testing coherent reflection in chinchilla: Auditory-nerve responses predict stimulus-frequency emissions. *J Acoust Soc Am* 124: 381–395.
23. Zweig G, Shera CA (1995) The origin of periodicity in the spectrum of evoked otoacoustic emissions. *J Acoust Soc Am* 98:2018–2047.
24. Bode H (1945) *Network Analysis and Feedback Amplifier Design* (Van Nostrand Reinhold, Princeton).
25. Oxenham AJ, Shera CA (2003) Estimates of human cochlear tuning at low levels using forward and simultaneous masking. *J Assoc Res Otolaryngol* 4:541–554.
26. Siegel JH, et al. (2005) Delays of stimulus-frequency otoacoustic emissions and cochlear vibrations contradict the theory of coherent reflection filtering. *J Acoust Soc Am* 118:2434–2443.
27. Ruggero MA, Temchin AN (2007) Similarity of traveling-wave delays in the hearing organs of humans and other tetrapods. *J Assoc Res Otolaryngol* 8:153–166.
28. Eustaquio-Martín A, Lopez-Poveda EA (2010) Isoresponse versus isoinput estimates of cochlear filter tuning. *J Assoc Res Otolaryngol* 12:281–299.
29. Puria S (2003) Measurements of human middle ear forward and reverse acoustics: Implications for otoacoustic emissions. *J Acoust Soc Am* 113:2773–2789.
30. Ruggero MA, Rich NC, Robles L, Shivapuja BG (1990) Middle-ear response in the chinchilla and its relationship to mechanics at the base of the cochlea. *J Acoust Soc Am* 87:1612–1629.
31. Songer JE, Rosowski JJ (2007) Transmission matrix analysis of the chinchilla middle ear. *J Acoust Soc Am* 122:932–942.
32. Fay RR (1988) *Hearing in Vertebrates: A Psychophysics Databook* (Hill–Fay Associates, Winnetka, IL).
33. Bitterman Y, Mukamel R, Malach R, Fried I, Nelken I (2008) Ultra-fine frequency tuning revealed in single neurons of human auditory cortex. *Nature* 451:197–201.
34. Bartlett EL, Sadagopan S, Wang X (2011) Fine frequency tuning in monkey auditory cortex and thalamus. *J Neurophysiol* 106:849–859.
35. Recanzone GH, Guard DC, Phan ML (2000) Frequency and intensity response properties of single neurons in the auditory cortex of the behaving macaque monkey. *J Neurophysiol* 83:2315–2331.
36. Heffner RS, Heffner HE (1992) Visual factors in sound localization in mammals. *J Comp Neurol* 317:219–232.
37. Ross CF (2000) Into the light: The origin of Anthropoidea. *Annu Rev Anthropol* 29: 147–194.
38. Rose JE, Hind JE, Anderson DJ, Brugge JF (1971) Some effects of stimulus intensity on response of auditory nerve fibers in the squirrel monkey. *J Neurophysiol* 34:685–699.
39. Rhode WS, Roth GL, Recio-Spinoso A (2010) Response properties of cochlear nucleus neurons in monkeys. *Hear Res* 259:1–15.
40. Martin GK, Lonsbury-Martin BL, Probst R, Coats AC (1988) Spontaneous otoacoustic emissions in a nonhuman primate. I. Basic features and relations to other emissions. *Hear Res* 33:49–68.
41. Bergevin C, et al. (2011) Stimulus-frequency otoacoustic emissions as a probe of cochlear tuning in the common marmoset. *Assoc Res Otolaryngol Abs* 34:371.
42. Eggermont JJ (1977) Compound action potential tuning curves in normal and pathological human ears. *J Acoust Soc Am* 62:1247–1251.
43. Harrison RV, Aran JM, Erre JP (1981) AP tuning curves from normal and pathological human and guinea pig cochleas. *J Acoust Soc Am* 69:1374–1385.
44. Harrison RV, Aran JM, Negrevergne M (1981) The frequency selectivity of the normal and pathological human cochlea. *Arch Otorhinolaryngol* 230:221–227.
45. Heinz MG, Colburn HS, Carney LH (2001) Evaluating auditory performance limits. I. One-parameter discrimination using a computational model for the auditory nerve. *Neural Comput* 13:2273–2316.
46. Recio A, Rhode WS, Kiefte M, Kluender KR (2002) Responses to cochlear normalized speech stimuli in the auditory nerve of cat. *J Acoust Soc Am* 111:2213–2218.
47. Kemp DT, Brass D, Souter M (1990) *Mechanics and Biophysics of Hearing*, eds Dallos P, Geisler CD, Matthews JW, Ruggero MA, Steele CR (Springer, New York), pp 202–209.
48. Guinan JJ (1990) *Mechanics and Biophysics of Hearing*, eds Dallos P, Geisler CD, Matthews JW, Ruggero MA, Steele CR (Springer, New York), pp 170–177.
49. Kalluri R, Shera CA (2007) Comparing stimulus-frequency otoacoustic emissions measured by compression, suppression, and spectral smoothing. *J Acoust Soc Am* 122: 3562–3575.
50. Louage DHG, van der Heijden M, Joris PX (2004) Temporal properties of responses to broadband noise in the auditory nerve. *J Neurophysiol* 91:2051–2065.
51. Mom T, Telischi FF, Martin GK, Stagner BB, Lonsbury-Martin BL (2000) Vasospasm of the internal auditory artery: Significance in cerebellopontine angle surgery. *Am J Otol* 21:735–742.